





New triple molybdate and tungstate $\text{Na}_5\text{Rb}_7\text{Sc}_2(\text{XO}_4)_9$ ($X = \text{Mo}, \text{W}$)

Tatyana S. Spiridonova ^{a*} , Aleksandra A. Savina ^{ab} ,
Evgeniy V. Kovtunets ^a , Elena G. Khaikina ^a 

a: Baikal Institute of Nature Management, Siberian Branch, Russian Academy of Sciences, 670047 Sakh'yanova st., 6, Ulan-Ude, Russia

b: Skolkovo Institute of Science and Technology, 121205 Bolshoy blvd., 30, Moscow, Russia

* Corresponding author: spiridonova-25@mail.ru

This article belongs to the regular issue.

© 2021, The Authors. This article is published in open access form under the terms and conditions of the Creative Commons Attribution (CC BY) license (<http://creativecommons.org/licenses/by/4.0/>).



Abstract

New compounds of the composition $\text{Na}_5\text{Rb}_7\text{Sc}_2(\text{XO}_4)_9$ ($X = \text{Mo}, \text{W}$) were obtained via the ceramic technology. The sequences of chemical transformations occurring during the formation of these compounds were established, and their primary characterization was performed. Both $\text{Na}_5\text{Rb}_7\text{Sc}_2(\text{XO}_4)_9$ ($X = \text{Mo}, \text{W}$) were found to melt incongruently at 857 K ($X = \text{Mo}$) and 889 K ($X = \text{W}$). They are isostructural to $\text{Ag}_5\text{Rb}_7\text{Sc}_2(\text{XO}_4)_9$ ($X = \text{Mo}, \text{W}$), $\text{Na}_5\text{Cs}_7\text{Ln}_2(\text{MoO}_4)_9$ ($\text{Ln} = \text{Tm}, \text{Yb}, \text{Lu}$) and crystallize in the trigonal crystal system (sp. gr. $R\bar{3}2$). The crystal structures were refined with the Rietveld method using the powder X-ray diffraction data. The thermal expansion of $\text{Na}_5\text{Rb}_7\text{Sc}_2(\text{WO}_4)_9$ was studied by high-temperature powder X-ray diffraction; it was shown that this triple tungstate belongs to high thermal expansion materials.

Keywords

sodium
rubidium
scandium
triple molybdate
triple tungstate
synthesis
crystal structure
thermal expansion

Received: 03.12.2021

Revised: 10.12.2021

Accepted: 14.12.2021

Available online: 16.12.2021

1. Introduction

The search for new functional inorganic materials based on the development of ideas about the relationships between their structure and properties is one of the high-priority directions of modern solid state chemistry, crystal chemistry and materials science. The greatest attention is paid to the synthesis, study of the structure and properties of complex oxides, among which binary Mo (VI) and W (VI) compounds of various compositions occupy a significant place. In the last two decades, triple molybdates have been actively studied, and in recent years, triple tungstates have also attracted much attention as interesting research objects. Constant interest in such compounds is maintained due to their wide range of functional properties, such as catalytic, luminescent, laser, nonlinear optical, ferroelectric, ion-conducting, and others. Thus, numerous publications are devoted to triple molybdates and tungstates with the $\text{BaNd}_2(\text{MoO}_4)_4$ -type structure, which are represented by two families of compounds: $\text{LiMR}_2(\text{MoO}_4)_4$ ($M = \text{K}, \text{Tl}, \text{Rb}$; $R = \text{Bi}, \text{Ln}$) and $\text{Li}_3\text{Ba}_2\text{Ln}_3(\text{XO}_4)_8$ ($X = \text{Mo}, \text{W}$). The prospects for possible application of these compounds as photo- and IR-phosphors, materials for UV

radiation dosimeters, laser materials are shown in [1–10]. The latter is also facilitated by the fact that the maximum anisotropy of thermal expansion in several representatives of this family is lower than that in other successfully used laser crystals [11]. The molybdate phosphor $\text{NaCaLa}(\text{MoO}_4)_3$: $\text{Tb}^{3+}/\text{Yb}^{3+}$ can be used as a spectral converter [12].

Triple molybdates $\text{Na}_5\text{Cs}_8\text{R}_5(\text{MoO}_4)_{24}$ ($R = \text{In}, \text{Sc}$ or Fe) [13, 14] and $\text{Na}_{10}\text{Cs}_4\text{Co}_5(\text{MoO}_4)_{12}$ [15], built on the basis of alluaudite $(\text{Na}, \text{Ca})\text{Mn}(\text{Fe}, \text{Mg})_2(\text{PO}_4)_3$, $M_{1-x}\text{A}_{1-x}\text{R}_{1+x}(\text{MoO}_4)_3$ [16, 17] with the NASICON-type structure, $\text{K}_5\text{ScHf}(\text{MoO}_4)_6$ [18] with the $\text{K}_5\text{InHf}(\text{MoO}_4)_6$ -type structure, and $\text{AgRb}_2\text{In}(\text{MoO}_4)_3$ [19], $\text{Ag}_3\text{Rb}_9\text{Sc}_2(\text{WO}_4)_9$ [20], $\text{Ag}_5\text{Rb}_7\text{Sc}_2(\text{XO}_4)_9$ ($X = \text{Mo}, \text{W}$) [21] that formed their own structural types are considered to be promising solid state electrolytes.

In this work, the family of triple molybdates and tungstates represented by formula $M'_5M''_7R_2(\text{XO}_4)_9$ [21, 22] is extended by two new compounds, $\text{Na}_5\text{Rb}_7\text{Sc}_2(\text{XO}_4)_9$ ($X = \text{Mo}, \text{W}$). The primary characterization of these phases was carried out. Their crystal structure was refined by the Rietveld method from powder X-ray diffraction data. In addition, the thermal expansion of $\text{Na}_5\text{Rb}_7\text{Sc}_2(\text{WO}_4)_9$ was studied.

2. Experimental

2.1. Preparation of materials

Commercially available chemically pure MoO₃, WO₃ (ReaKhim, Ltd, Russia), AgNO₃ (KhimKo, Ltd, Russia) and high purity Sc₂O₃ (SibMetallTorg, Ltd, Russia), Rb₂CO₃ (Sigma-Aldrich, China) were used as starting materials for preparing molybdates and tungstates. Rb₂XO₄ (*X* = Mo, W) was prepared by high temperature annealing of a stoichiometric mixture of Rb₂CO₃ and XO₃ (723–823 K, 80 h). Sc₂(XO₄)₃ (*X* = Mo, W) was obtained from Sc₂O₃ and XO₃ (*X* = Mo, 773–1023 K, 80 h; *X* = W, 773–1123 K, 80 h). Anhydrous Na₂XO₄ (*X* = Mo, W) used in this work were obtained by calcining the corresponding crystalline hydrates at 823–873 K.

The phase purity of the prepared samples was confirmed by powder X-ray diffraction (PXRD). The PXRD patterns of Na₂XO₄, Rb₂XO₄, Sc₂(XO₄)₃ (*X* = Mo, W) were in good agreement with the literature data [23].

2.2. Instrumental characterization methods

The processes that occur during the solid-state syntheses were monitored with PXRD using a D8 ADVANCE Bruker diffractometer (VANTEC detector, Cu K α radiation, λ = 1.5418 Å, reflection geometry, secondary monochromator). High temperature X-ray measurements of Na₅Rb₇Sc₂(WO₄)₉ were performed with the same instrument using an Anton Paar HTK 16 high temperature chamber in the temperature range of 303–823 K. The heating rate was 20 K min⁻¹. Prior to measurements, the sample was kept at a specified temperature for 25 min.

The unit cell parameters of Na₅Rb₇Sc₂(XO₄)₉ (*X* = Mo, W) were refined by the least-squares method using ICDD program package for preparing experimental standards. The Smith–Snyder F30 criterion was used as a validation criterion for X-ray patterns indexing [24]. The crystal structures refinement of Na₅Rb₇Sc₂(XO₄)₉ (*X* = Mo, W) at room temperature and the unit cell parameters determination in high-temperature studies were carried out by the Rietveld method [25] using the TOPAS 4.2 software [26].

The thermal measurements were carried out using an STA 449 F1 Jupiter NETZSCH thermoanalyser (Pt crucible, heating rate of 10 K min⁻¹ in a flow of argon).

3. Results and discussion

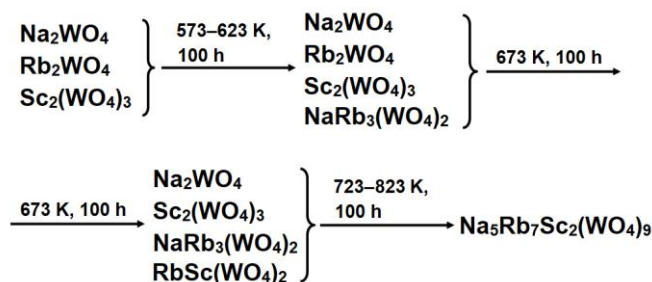
3.1. Synthesis and characterization of

Na₅Rb₇Sc₂(XO₄)₉ (*X* = Mo, W)

Polycrystalline Na₅Rb₇Sc₂(XO₄)₉ (*X* = Mo, W) were synthesized by annealing the stoichiometric mixtures of Na₂XO₄, Rb₂XO₄ and Sc₂(XO₄)₃ at 773–823 K for 80 h (*X* = Mo), 100 h (*X* = W).

The final powder products are of white color, insoluble in water and common organic solvents, soluble in HCl (Na₅Rb₇Sc₂(MoO₄)₉ at room temperature, Na₅Rb₇Sc₂(WO₄)₉ – at heating).

According to the results of PXRD data, the sequence of chemical transformations in the course of Na₅Rb₇Sc₂(WO₄)₉ formation from a stoichiometric mixture of simple tungstates can be illustrated by the following scheme:



Scheme 1 The sequence of chemical transformations in the course of Na₅Rb₇Sc₂(WO₄)₉ formation

In the Mo-containing system the formation of Na₅Rb₇Sc₂(MoO₄)₉ started at the stage when NaRb₃(MoO₄)₂ and RbSc(MoO₄)₂ appeared. The corresponding scheme differs from that for ternary tungstate only in shorter synthesis times.

Both Mo- and W-based Na₅Rb₇Sc₂(XO₄)₉ melt incongruently at 857 K (*X* = Mo) and 889 K (*X* = W) (Fig. 1). Reflections of both NaSc(MoO₄)₂ and a phase with an alluaudite-type structure together with the initial phase were found in the PXRD pattern of the cooled Na₅Rb₇Sc₂(MoO₄)₉ melt. The cooled melt of Na₅Rb₇Sc₂(WO₄)₉ contains the double tungstates RbSc(WO₄)₂ and NaSc(WO₄)₂ and an alluaudite-like phase. The amount of the latter phase was dominant.

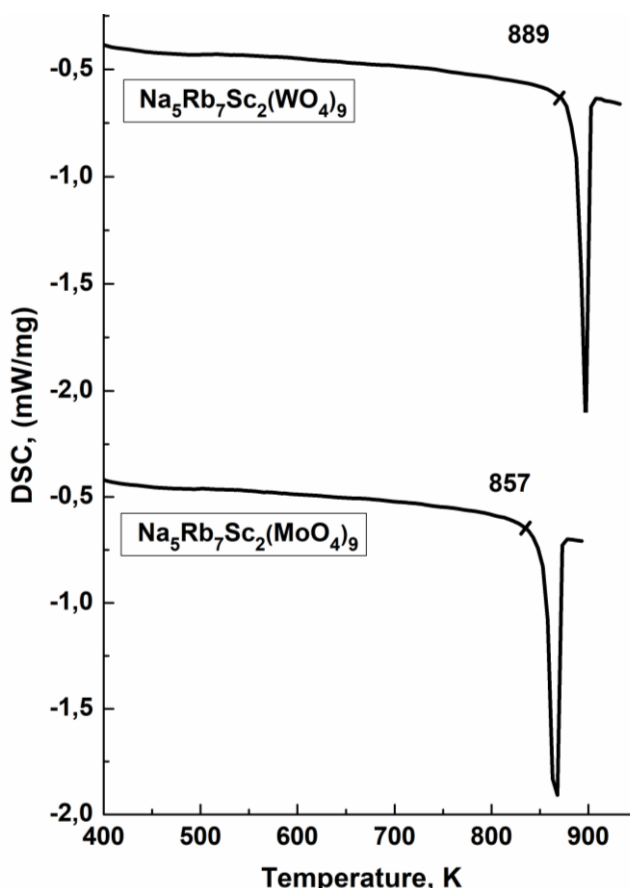


Fig. 1 The DSC curves for polycrystalline Na₅Rb₇Sc₂(XO₄)₉ (*X* = W, Mo)

The PXRD patterns of prepared single-phase compounds $\text{Na}_5\text{Rb}_7\text{Sc}_2(\text{XO}_4)_9$ ($X = \text{Mo}, \text{W}$) are similar and show that these complex oxides are isostructural to trigonal $\text{Na}_5\text{Cs}_7\text{Yb}_2(\text{MoO}_4)_9$, $\text{Ag}_5\text{Rb}_7\text{Sc}_2(\text{XO}_4)_9$ ($X = \text{Mo}, \text{W}$) (sp. gr. $R\bar{3}2, Z = 3$) [21, 22]. This allows satisfactorily indexing the PXRD patterns of $\text{Na}_5\text{Rb}_7\text{Sc}_2(\text{XO}_4)_9$ ($X = \text{Mo}, \text{W}$) (in the case of molybdate $F(3\sigma) = 141.6$ (0.0056; 38), for tungstate $F(3\sigma) = 287.2$ (0.0028; 37)). The obtained crystallo-

graphic characteristics are shown in Table 1, the results of indexing of $\text{Na}_5\text{Rb}_7\text{Sc}_2(\text{WO}_4)_9$ are shown in Table 2 as an example.

Table 1 Unit cell parameters for $\text{Na}_5\text{Rb}_7\text{Sc}_2(\text{XO}_4)_9$ ($X = \text{Mo}, \text{W}$)

X	$a, \text{Å}$	$c, \text{Å}$	$V, \text{Å}^3$
Mo	10.1264(1)	35.6570(7)	3172.80
W	10.1899(2)	35.6096(9)	3202.12

Table 2 The PXRD data for $\text{Na}_5\text{Rb}_7\text{Sc}_2(\text{WO}_4)_9$

$h k l$	$2\theta_{\text{exp}}, ^\circ$	I/I_0	$d_{\text{exp}}, \text{Å}$	$\Delta = 2\theta_{\text{exp}} - 2\theta_{\text{calc}}, ^\circ$	$h k l$	$2\theta_{\text{exp}}, ^\circ$	I/I_0	$d_{\text{exp}}, \text{Å}$	$\Delta = 2\theta_{\text{exp}} - 2\theta_{\text{calc}}, ^\circ$
1 0 1	10.322	1	8.563	-0.003	2 1 13	42.680	3	2.1167	-0.002
0 1 2	11.183	2	7.906	-0.002	0 4 5	42.879	2	2.1074	+0.000
1 0 4	14.117	1L	6.268	+0.003	3 0 12	43.273	2	2.0891	+0.000
0 0 6	14.911	1L	5.936	+0.004	0 1 17	44.418	1L	2.0379	-0.005
0 1 5	15.974	1L	5.544	+0.004	4 0 7	44.739	2	2.0240	-0.001
1 1 0	17.390	20	5.095	+0.001	1 2 14	44.781	2	2.0222	-0.009
1 1 3	18.938	42	4.682	+0.001	3 2 1	44.813	2	2.0208	-0.011
1 0 7	20.131	1	4.407	+0.000	1 3 10	44.914	1	2.0165	-0.013
0 2 1	20.264	1	4.379	-0.001	2 3 2	45.033	1	2.0114	-0.003
2 0 2	20.724	2	4.283	-0.001	0 2 16	45.615	1L	1.9871	+0.000
0 0 9	22.454	13	3.9563	-0.002	0 0 18	45.831	7	1.9783	-0.001
1 1 6	22.987	100	3.8658	+0.000	3 2 4	45.930	1	1.9742	+0.002
2 0 5	23.694	1	3.7520	+0.007	3 1 11	46.475	2	1.9523	+0.000
0 2 7	26.722	2	3.3333	+0.001	2 3 5	46.604	1	1.9472	-0.004
2 1 1	26.824	15	3.3209	+0.000	2 2 12	46.970	2	1.9329	+0.000
1 0 10	26.973	1L	3.3029	+0.005	4 1 0	47.157	3	1.9257	-0.001
1 2 2	27.178	3	3.2784	+0.000	4 1 3	47.813	5	1.9008	-0.002
1 1 9	28.541	59	3.1249	-0.001	2 0 17	48.045	1L	1.8921	-0.004
0 1 11	29.345	2	3.0411	+0.018	3 2 7	48.348	2	1.8810	-0.001
1 2 5	29.546	5	3.0208	+0.002	4 0 10	48.505	1L	1.8753	-0.004
0 0 12	30.094	1	2.9671	-0.004	2 1 16	49.167	1L	1.8516	+0.007
0 3 0	30.362	54	2.9415	-0.001	3 0 15	49.280	1L	1.8476	+0.005
3 0 3	31.304	1	2.8551	-0.001	1 1 18	49.379	5	1.8441	-0.002
2 1 7	32.067	2	2.7889	-0.006	2 3 8	49.422	1	1.8426	-0.008
1 2 8	33.548	3	2.6690	-0.002	4 1 6	49.737	8	1.8317	-0.001
3 0 6	33.989	5	2.6354	-0.002	1 3 13	49.930	1	1.8250	-0.002
2 0 11	34.335	1L	2.6096	-0.006	0 4 11	49.993	2	1.8229	-0.006
1 1 12	34.964	15	2.5641	-0.002	1 2 17	51.478	2	1.7737	-0.005
2 2 0	35.200	5	2.5475	+0.000	3 1 14	51.749	1L	1.7651	+0.045
2 2 3	36.031	1	2.4906	-0.002	0 5 1	51.820	1L	1.7628	+0.001
0 1 14	36.738	1L	2.4443	+0.004	3 2 10	51.916	1	1.7598	-0.006
1 3 1	36.779	2	2.4417	-0.002	2 2 15	52.659	4	1.7367	-0.002
2 1 10	36.898	1L	2.4340	-0.004	4 1 9	52.831	15	1.7314	-0.002
3 1 2	37.057	1L	2.4240	-0.012	0 2 19	53.025	1	1.7256	+0.018
3 0 9	38.091	6	2.3605	-0.002	4 0 13	53.279	1	1.7179	-0.009
2 2 6	38.423	8	2.3409	-0.001	2 3 11	53.336	1	1.7162	-0.009
3 1 5	38.875	2	2.3147	+0.001	3 3 0	53.946	5	1.6983	-0.002
1 3 7	40.884	1	2.2055	-0.001	3 3 3	54.538	2	1.6812	+0.001
4 0 1	40.950	1	2.2021	+0.002	0 5 7	55.016	1L	1.6677	+0.011
0 4 2	41.201	1	2.1892	-0.004	2 4 1	55.077	2	1.6660	+0.005
1 0 16	41.799	1L	2.1593	+0.025	4 2 2	55.268	1L	1.6607	+0.010
1 1 15	41.952	9	2.1518	-0.002	1 3 16	55.766	1L	1.6471	+0.017
2 2 9	42.156	19	2.1418	-0.002	3 0 18	55.969	13	1.6416	-0.001

Cu $K\alpha_1$ radiation ($\lambda = 1.54056 \text{ Å}$)

3.2. Rietveld refinement of $\text{Na}_5\text{Rb}_7\text{Sc}_2(\text{XO}_4)_9$ ($X = \text{Mo}, \text{W}$) structure

The positional atomic parameters for the $\text{Ag}_5\text{Rb}_7\text{Sc}_2(\text{MoO}_4)_9$ structure [21] were taken as a starting model for the refinement of the $\text{Na}_5\text{Rb}_7\text{Sc}_2(\text{XO}_4)_9$ ($X = \text{Mo}, \text{W}$) structures by the Rietveld method. The refinement was carried out by gradually adding the refined parameters with the simultaneous graphical simulation of the background. The Pearson VII Function was used to describe the shape of peaks. Isotropic displacement parameters (B_{iso}) for all atoms in $\text{Na}_5\text{Rb}_7\text{Sc}_2(\text{MoO}_4)_9$ were refined separately, while for the O atoms in $\text{Na}_5\text{Rb}_7\text{Sc}_2(\text{WO}_4)_9$ they were taken as equal. The refinement procedure included corrections for the sample preferred orientation and broadening of peaks due to anisotropy within the model of spherical harmonics [27]. The refinement results for $\text{Na}_5\text{Rb}_7\text{Sc}_2(\text{XO}_4)_9$ ($X = \text{Mo}, \text{W}$) are shown in Table 3. Experimental, theoretical and difference PXRD patterns for $\text{Na}_5\text{Rb}_7\text{Sc}_2(\text{XO}_4)_9$ ($X = \text{Mo}, \text{W}$) are shown in Fig. 2 and 3. The fractional atomic coordinates, isotropic atomic displacement parameters, cation occupancies and main selected interatomic distances are presented in Tables 4–7.

The crystal structures of $\text{Na}_5\text{Rb}_7\text{Sc}_2(\text{MoO}_4)_9$ and $\text{Na}_5\text{Rb}_7\text{Sc}_2(\text{WO}_4)_9$ were deposited in the Cambridge Crystallographic Data Centre with Cambridge Structural Database (CSD) N° 2124713 and N° 2124691, respectively [28].

Table 3 Main structure parameters for $\text{Na}_5\text{Rb}_7\text{Sc}_2(\text{XO}_4)_9$ ($X = \text{Mo}, \text{W}$) after the Rietveld refinement

Compound	$\text{Na}_5\text{Rb}_7\text{Sc}_2(\text{MoO}_4)_9$	$\text{Na}_5\text{Rb}_7\text{Sc}_2(\text{WO}_4)_9$
Sp. gr.	$R\bar{3}2$	$R\bar{3}2$
a , Å	10.13752(9)	10.19247(9)
c , Å	35.6615(4)	35.6191(4)
V , Å ³	3173.91(7)	3204.59(7)
Z	3	3
2θ -interval, °	8–100	8–100
R_{wp} , %	4.15	4.56
R_p , %	3.20	3.42
R_{exp} , %	2.04	1.81
χ^2	2.04	2.51
R_B , %	1.64	2.11

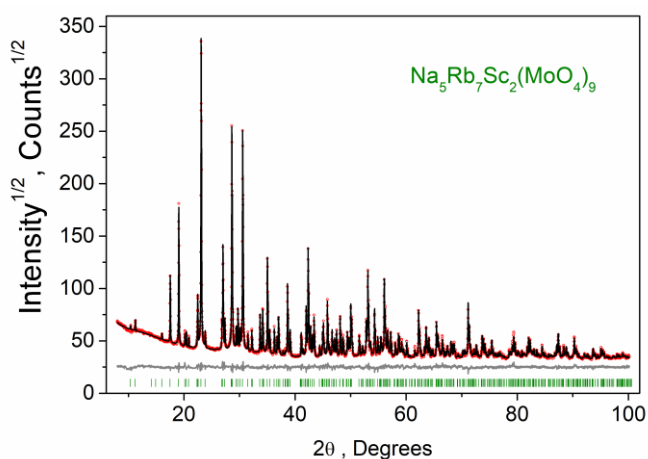


Fig. 2 Observed, calculated and difference diffractograms of $\text{Na}_5\text{Rb}_7\text{Sc}_2(\text{MoO}_4)_9$

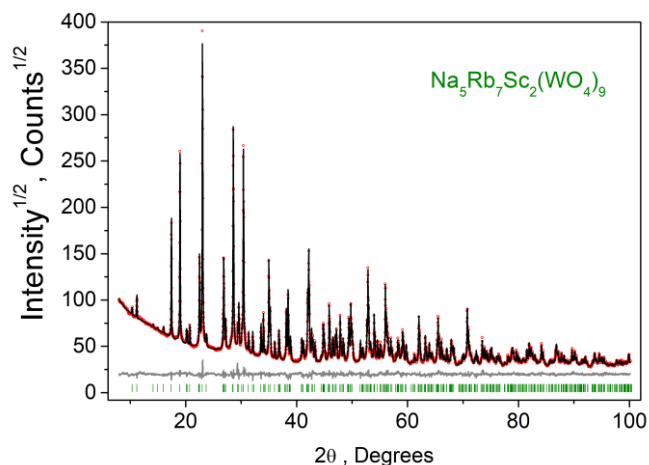


Fig. 3 Observed, calculated and difference diffractograms of $\text{Na}_5\text{Rb}_7\text{Sc}_2(\text{WO}_4)_9$

In the structures of $\text{Na}_5\text{Rb}_7\text{Sc}_2(\text{XO}_4)_9$ ($X = \text{Mo}, \text{W}$), Na1 and Na2 atoms are located in threefold special positions with the point symmetry $3\bar{2}$; Sc, Rb1, and Rb2 sit at threefold axes; Rb3, Mo2 (W2), and Na3 are settled at twofold axes, and Mo1 (W1) and oxygen atoms are in general positions. Both Mo and W atoms have tetrahedral coordination, while Sc, Na1 and Na3 possess octahedral coordination. It is worth noting that, unlike the octahedron surrounding Na1, the octahedron around Na3 is distorted. The half-occupied Na2 site has a trigonal-prismatic environment. Rb1 and Rb2 atoms have 9-fold environments, while Rb3 exhibits CN = 8. The general view of the structure is illustrated in Fig. 4a.

The characteristic details of the title compounds are so-called 'lanterns' [$\text{Sc}_2(\text{XO}_4)_9$] ($X = \text{Mo}, \text{W}$) composed by two ScO_6 octahedra sharing corners with six terminal and three bridging XO_4 tetrahedra (Fig. 4b). Together with the Rb1, Rb2 and Na3 cations they form two-tiered hexagonal layers parallel to (001) plane, which resemble the motif of the $\text{K}_3\text{Na}(\text{SO}_4)_2$ glaserite structure [29]. The layers are folded with a displacement along the b axis and are connected by Na3, Na1 and Rb3 cations (Fig. 4c).

Similar "lanterns" [$M_2(\text{TO}_4)_9$] (M is an octahedrally coordinated cation, TO_4 is a tetrahedral oxoanion), and hexagonal layers formed by them also characterize the structures of previously studied $\text{Ag}_5\text{Rb}_7\text{Sc}_2(\text{MoO}_4)_9$, $\text{Ag}_5\text{Rb}_7\text{Sc}_2(\text{WO}_4)_9$ and $\text{Na}_5\text{Cs}_7\text{Yb}_2(\text{MoO}_4)_9$ [21]. The relationship between structure of the considered family $M'_5M''_7R_2(\text{XO}_4)_9$ ($X = \text{Mo}, \text{W}$) and many rhombohedral triple molybdates and tungstates with $a = 9\text{--}10$ Å and large c -periods (more than 20 Å) was discussed in [21].

3.3. Thermal expansion of $\text{Na}_5\text{Rb}_7\text{Sc}_2(\text{WO}_4)_9$

The thermal expansion of $\text{Na}_5\text{Rb}_7\text{Sc}_2(\text{WO}_4)_9$ was studied by high-temperature X-ray diffraction. The thermal expansion of this compound, which crystallizes in a trigonal symmetry, is defined by two linear thermal expansion coefficients (LTECs) measured along (α_c) and across (α_a) the threefold axis. The average LTEC can be calculated as follows: $\alpha_{\text{av}} = \alpha_v/3 = (2\alpha_a + \alpha_c)/3$. Thermal expansion anisotropy is quantitatively defined as $|\alpha_a - \alpha_c|$.

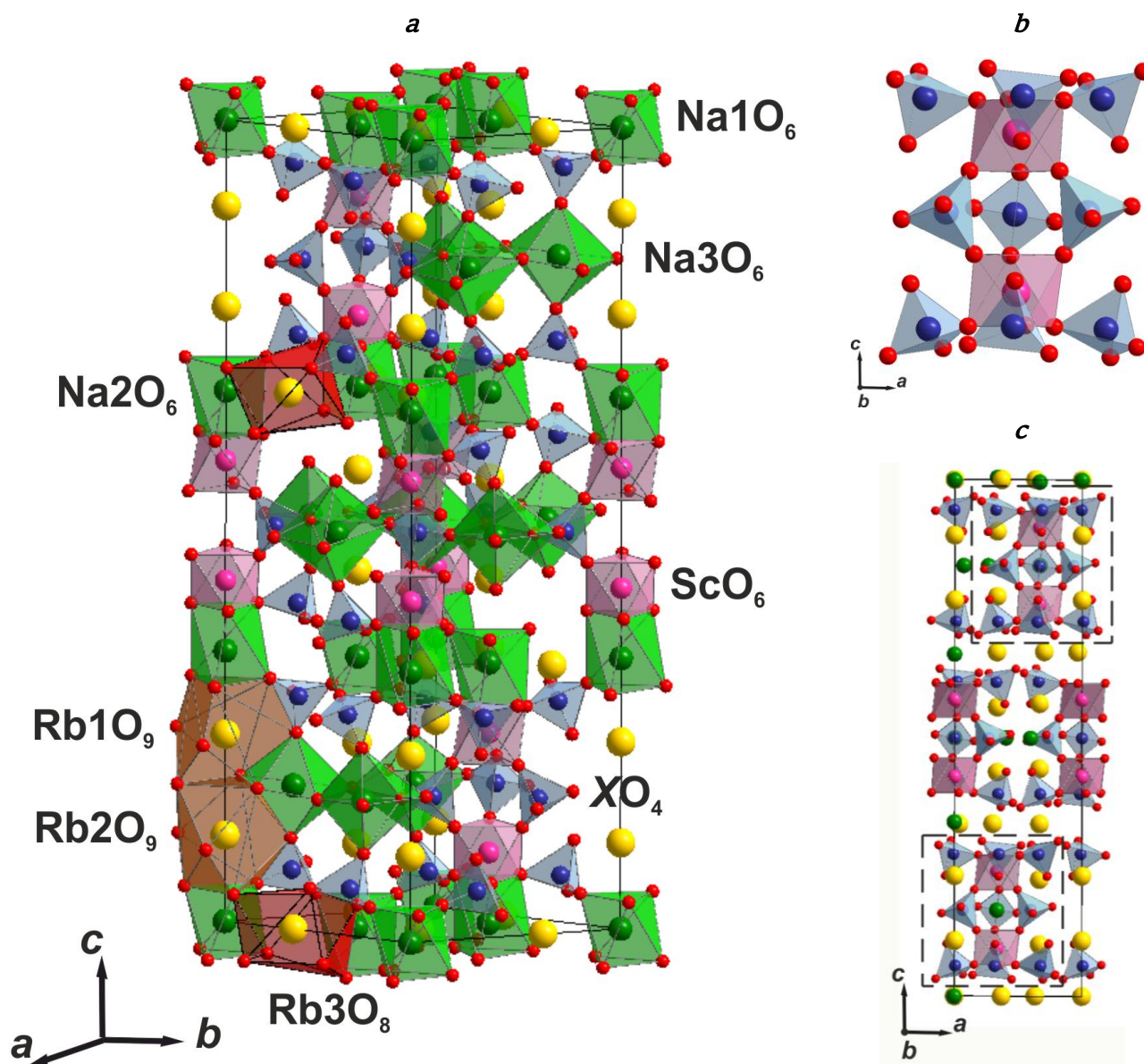


Fig. 4 The crystal structure of $\text{Na}_5\text{Rb}_7\text{Sc}_2(\text{XO}_4)_9$ ($X = \text{Mo}, \text{W}$): a general view (a); $[\text{Sc}_2(\text{XO}_4)_9]$ cluster (b); layers of $[\text{Sc}_2(\text{XO}_4)_9]$ clusters (c)

Table 4 Fractional atomic coordinates and isotropic displacement parameters (\AA^2) for $\text{Na}_5\text{Rb}_7\text{Sc}_2(\text{MoO}_4)_9$

Atom	<i>x</i>	<i>y</i>	<i>z</i>	<i>B</i> _{iso}	<i>Occ.</i>
Rb1	0	0	0.2332(1)	1.9 (1)	1
Rb2	0	0	0.1074(1)	2.0(1)	1
Rb3	0	0.3687(3)	0	4.6(2)	1
Na1	0	0	0	1.9(6)	1
Na2	0	0	0.3376(8)	2.1(3)	0.5
Na3	0.4030(9)	0.4030(9)	0.5	2.1(3)	1
Sc2	0	0	0.4253(3)	2.1(2)	1
Mo1	0.3429(2)	0.3265(3)	0.39176(4)	1.30(9)	1
Mo2	0.7331(2)	0.7331(2)	0.5	0.9(1)	1
O1	0.458(1)	0.269(1)	0.3746(4)	3.2(4)	1
O2	0.362(1)	0.480(1)	0.3662(3)	1.4(4)	1
O3	0.406(1)	0.394(1)	0.4344(3)	0.4(3)	1
O4	0.147(1)	0.180(1)	0.3938(3)	1.8(2)	1
O5	0.566(1)	0.719(1)	0.4937(4)	1.6(4)	1
O6	0.822(1)	0.839(2)	0.5391(3)	1.8(2)	1

Table 5 Fractional atomic coordinates and isotropic displacement parameters (\AA^2) for $\text{Na}_5\text{Rb}_7\text{Sc}_2(\text{WO}_4)_9$

Atom	<i>x</i>	<i>y</i>	<i>z</i>	<i>B</i> _{iso}	<i>Occ.</i>
Rb1	0	0	0.2331(2)	1.1(2)	1
Rb2	0	0	0.1083(2)	1.7(2)	1
Rb3	0	0.3671(5)	0	3.1(2)	1
Na1	0	0	0	2(1)	1
Na2	0	0	0.329(2)	3(1)	0.5
Na3	0.418(1)	0.418(1)	0.5	4.3(6)	1
Sc2	0	0	0.4241(3)	0.5(3)	1
W1	0.3410(1)	0.3251(1)	0.39174(3)	0.8(1)	1
W2	0.7329 (1)	0.7329(1)	0.5	0.9(1)	1
O1	0.4660(7)	0.2580(8)	0.3785(3)	1.0(2)	1
O2	0.376(1)	0.4839(7)	0.3633(2)	1.0(2)	1
O3	0.4104(8)	0.3974(9)	0.4371(2)	1.0(2)	1
O4	0.1487(9)	0.1765(9)	0.3976(4)	1.0(2)	1
O5	0.5570(8)	0.7196(7)	0.4896(2)	1.0(2)	1
O6	0.823(1)	0.840(1)	0.5412(2)	1.0(2)	1

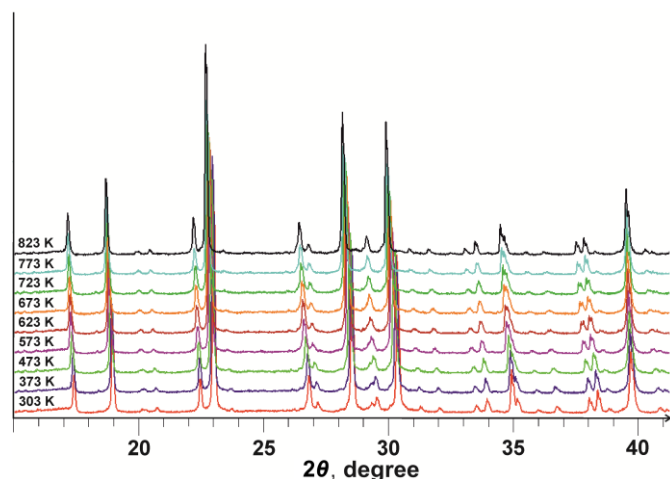
Table 6 Main bond lengths (Å) in $\text{Na}_5\text{Rb}_7\text{Sc}_2(\text{MoO}_4)_9$

Mo1-tetrahedron		Mo2-tetrahedron		Sc-octahedron	
Mo1-O1	1.660(9)	Mo2-O5	1.64(1) (× 2)	Sc-O4	2.02(1) (× 3)
-O2	1.73(1)	-O6	1.71(1) (× 2)	-O6	2.14(1) (× 3)
-O3	1.66(1)	<Mo2-O>	1.67	<Sc-O>	2.08
-O4	1.79(1)				
<Mo1-O>	1.71				
Na1-octahedron		Na2-trigonal prism		Na3-octahedron	
Na1-O1	2.39(1) (× 6)	Na2-O2	2.45(2) (× 3)	Na3-O3	2.34(1) (× 2)
		-O4	2.62(2) (× 3)	-O5	2.192(9) (× 2)
		<Na2-O>	2.53	-O5'	2.78(1) (× 2)
				<Na3-O>	2.44
Rb1-polyhedron		Rb2-polyhedron		Rb3-polyhedron	
Rb1-O5	3.04(1) (× 3)	Rb2-O5	3.18(1) (× 3)	Rb3-O1	3.05(1) (× 2)
-O3	3.20(1) (× 3)	-O3	3.00(1) (× 3)	-O2	3.00(1) (× 2)
-O2	3.16(1) (× 3)	-O1	3.01(1) (× 3)	-O2'	3.11(1) (× 2)
<Rb1-O>	3.13	<Rb2-O>	3.06	-O4	3.18(1) (× 2)
				<Rb3-O>	3.08

Table 7 Main bond lengths (Å) of $\text{Na}_5\text{Rb}_7\text{Sc}_2(\text{WO}_4)_9$

W1-tetrahedron		W2-tetrahedron		Sc-octahedron	
W1-O1	1.785(5)	W2-O5	1.768(6) (× 2)	Sc-O4	1.92(1) (× 3)
-O2	1.788(7)	-O6	1.786(8) (× 2)	-O6	2.12(1) (× 3)
-O3	1.771(8)	<W2-O>	1.777	<Sc-O>	2.02
-O4	1.792(7)				
<W1-O>	1.784				
Na1-octahedron		Na2-trigonal prism		Na3-octahedron	
Na1-O1	2.406(9) (× 6)	Na2-O2	2.30(2) (× 3)	Na3-O3	2.247(8) (× 2)
		-O4	2.96(5) (× 3)	-O5	2.76(1) (× 2)
		<Na2-O>	2.63	-O5'	2.69(1) (× 2)
				<Na3-O>	2.57
Rb1-polyhedron		Rb2-polyhedron		Rb3-polyhedron	
Rb1-O5	2.870(8) (× 3)	Rb2-O5	3.202(9) (× 3)	Rb3-O1	3.043(9) (× 2)
-O3	3.212(8) (× 3)	-O3	2.997(7) (× 3)	-O2	2.874(9) (× 2)
-O2	3.27(1) (× 3)	-O1	2.88(1) (× 3)	-O2'	3.209(9) (× 2)
<Rb1-O>	3.12	<Rb2-O>	3.03	-O4	3.32(1) (× 2)
				<Rb3-O>	3.11

The reflections in the X-ray diffraction patterns of $\text{Na}_5\text{Rb}_7\text{Sc}_2(\text{WO}_4)_9$ regularly shift with increasing temperature (Fig. 5) due to an increase in the unit cell parameters (Fig. 6).

**Fig. 5** Fragments of $\text{Na}_5\text{Rb}_7\text{Sc}_2(\text{WO}_4)_9$ diffractograms from 303 K to 823 K

The parameter a changes with temperature almost linearly; the temperature variation of the parameter c is described by a polynomial of the second degree (Table 8). Table 8 also presents the coefficients of thermal linear expansion and thermal expansion anisotropy. The obtained results allowed classifying $\text{Na}_5\text{Rb}_7\text{Sc}_2(\text{WO}_4)_9$ as belonging to high thermal expansion materials.

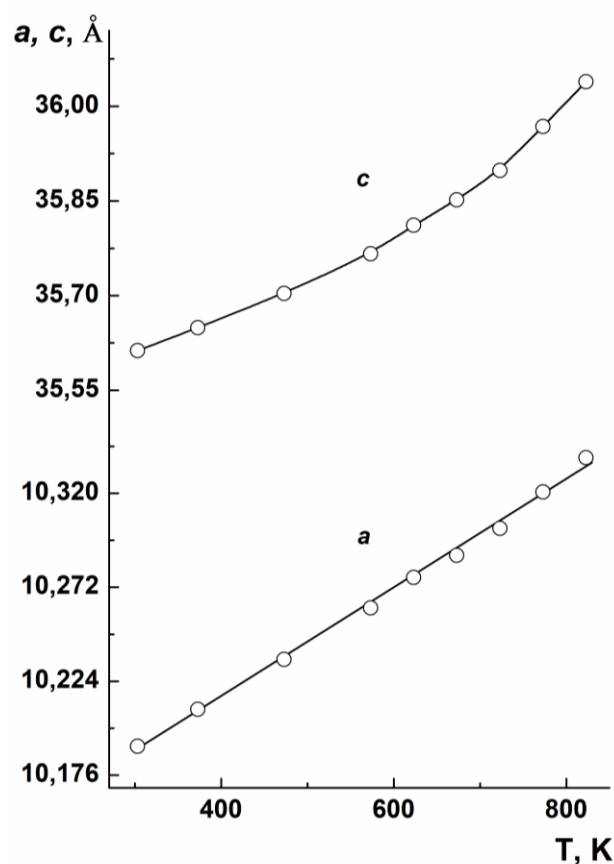
4. Conclusions

Two new compounds $\text{Na}_5\text{Rb}_7\text{Sc}_2(\text{XO}_4)_9$ ($X = \text{Mo}, \text{W}$) were obtained by a solid-phase synthesis, supplementing the previously discovered family of isostructural triple molybdates and tungstates of the composition $M_7M''_5R_2(\text{XO}_4)_9$. The thermal stability of obtained compounds was studied and the thermal expansion of $\text{Na}_5\text{Rb}_7\text{Sc}_2(\text{WO}_4)_9$ was examined by the high-temperature XRD diffraction method; it was shown that this compound belongs to highly expanding substances. The crystal structure of $\text{Na}_5\text{Rb}_7\text{Sc}_2(\text{XO}_4)_9$ ($X = \text{Mo}, \text{W}$) was refined by the Rietveld method using the PXRD data.

Table 8 Fitting polynomials for temperature dependent LTECs and average LTECs for $\text{Na}_5\text{Rb}_7\text{Sc}_2(\text{WO}_4)_9$ in the temperature range 303–823 K

Composition	Polynomials for $a(T)$ and $c(T)$, Å	LTEC·10 ⁻⁶ , K ⁻¹			
		α_a	α_c	α_{aV}	$ \alpha_a - \alpha_c $
$\text{Na}_5\text{Rb}_7\text{Sc}_2(\text{WO}_4)_9$	$a = 0.0003T + 10.18$ $c = 1 \times 10^{-6}T^2 + 0.0002T + 35.612$	27.8(3)	22.9(2)	26.2(3)	4.9

The obtained compounds crystallize in the chiral sp. gr. $R32$ and together with their formula and structural analogues $\text{Ag}_5\text{Rb}_7\text{Sc}_2(\text{XO}_4)_9$ ($X = \text{Mo}, \text{W}$), $\text{Na}_5\text{Cs}_7\text{Ln}_2(\text{MoO}_4)_9$ ($\text{Ln} = \text{Tm}, \text{Yb}, \text{Lu}$) belong to the series of rhombohedral triple molybdates and tungstates with $a = 9\text{--}10$ Å and long c -parameter, more than 20 Å; many of those have noticeable ionic conductivity at elevated temperatures [19–21]. For two representatives of the $M'_7M''_5R_2(\text{XO}_4)_9$ family, namely, $\text{Ag}_5\text{Rb}_7\text{Sc}_2(\text{XO}_4)_9$ ($X = \text{Mo}, \text{W}$), we confirmed this experimentally earlier [21]. This stimulates our research to find new representatives of this group of phases, as well as to continue the study of the ion-conducting properties of already obtained compounds – $(\text{Na}_5\text{Rb}_7\text{Sc}_2(\text{XO}_4)_9)$ ($X = \text{Mo}, \text{W}$) and $\text{Na}_5\text{Cs}_7\text{Ln}_2(\text{MoO}_4)_9$ ($\text{Ln} = \text{Tm}, \text{Yb}, \text{Lu}$). In addition, it seems expedient to carry out a further study of thermophysical properties for representatives of the considered structural type to reveal the influence of the nature of one-, three- and hexavalent elements on the value of thermal expansion coefficients and anisotropy in these phases.

**Fig. 6** Temperature dependences of the a and c unit cell parameters for $\text{Na}_5\text{Rb}_7\text{Sc}_2(\text{WO}_4)_9$

Acknowledgments

This work was financially supported by the Russian Foundation for Basic Research, project № 20-03-00533 (synthesis and research of $\text{Na}_5\text{Rb}_7\text{Sc}_2(\text{WO}_4)_9$) and by the Ministry of Science and Higher Education of the Russian Federation, Basic Project of BINM SB RAS № 0273-2021-0008 (synthesis and research of $\text{Na}_5\text{Rb}_7\text{Sc}_2(\text{MoO}_4)_9$). X-ray powder diffraction and thermal analysis results were obtained using the equipment of the Collective Use Center BINM SB RAS.

References

- Morozov VA, Lazoryak BI, Smirnov VA, Mikhailin VV, Basovich OM, Khaikina EG. Crystal structures and luminescence properties of triple molybdates $\text{LiMNd}_2(\text{MoO}_4)_4$ ($M = \text{K}, \text{Rb}, \text{Tl}$). Russ J Inorg Chem. 2001;46(6):873–879.
- Song M, Zhang L, Wang G. Growth and spectral properties of Nd^{3+} -doped $\text{Li}_3\text{Ba}_2\text{Ln}_3(\text{MoO}_4)_8$ ($\text{Ln} = \text{La}, \text{Gd}$) crystals. J Alloys Compds. 2009;480:839–842. doi:10.1016/j.jallcom.2009.02.082
- Xie A, Yuan XM, Wang FX. A potential red-emitting phosphors scheelite-like triple molybdates $\text{LiKGd}_2(\text{MoO}_4)_4$: Eu^{3+} for white light emitting diode applications. Sci China Tech Sci. 2011;54:70–75. doi:10.1007/s11431-010-4222-y
- Li H, Zhang L, Wang G. Growth, structure and spectroscopic characterization of a new laser crystals $\text{Nd}^{3+}:\text{Li}_3\text{Ba}_2\text{Gd}_3(\text{WO}_4)_8$. J Alloys Compd. 2009;478(1):484–488. doi:10.1016/j.jallcom.2008.11.079
- Xiao B, Lin Zh, Zhang L, Huang Y, Wang G. Growth, thermal and spectral properties of Er^{3+} -doped and $\text{Er}^{3+}/\text{Yb}^{3+}$ -codoped $\text{Li}_3\text{Ba}_2\text{La}_3(\text{WO}_4)_8$ crystals. PLoS ONE. 2012;7(7):40631. doi:10.1371/journal.pone.0040631
- Pan Yu, Chen Y, Lin Y, Gong X, Huang J, Luo Z, Huang YD. Structure, spectral properties and laser performance of Tm^{3+} -doped $\text{Li}_3\text{Ba}_2\text{La}_3(\text{WO}_4)_8$ crystal. Cryst Eng Comm. 2012;14:3930–3935. doi:10.1039/C2CE25190F
- Li H, Lin Zh, Zhang L, Huang Y, Wang G. Spectroscopic characteristics of Yb^{3+} -doped $\text{Li}_3\text{Ba}_2\text{Y}_3(\text{WO}_4)_8$ crystal. J Lumin. 2012;132:1507–1510. doi:10.1016/j.jlumin.2012.01.050
- Hu J, Gong X, Huang J, Chen Yu, Lin Y, Luo Z, Huang YD. Near ultraviolet excited Eu^{3+} doped $\text{Li}_3\text{Ba}_2\text{La}_3(\text{WO}_4)_8$ red phosphors for white light emitting diodes. Opt Mater Express. 2016;6:181. doi:10.1364/OME.6.000181
- Zeng X-L, Zhang J-Y, Chen D-G, Huang F. Crystal Structure and Spectroscopic Properties of a New Ternary Tungstate $\text{Li}_3\text{Ba}_2\text{Ho}_3(\text{WO}_4)_8$. Chin J Struct Chem. 2013;1:33–38.
- Guo W, Jiao Y, Wang P, Liu Q, Liu Sh, Hou F. Energy transfer and spectroscopic characterization of new green emitting $\text{Li}_3\text{Ba}_2\text{Gd}_3(\text{WO}_4)_8:\text{Tb}^{3+}$ phosphor. Solid State Phenom. 2018;281:686–691. doi:10.4028/www.scientific.net/SSP.281.686
- Han X, Calderon R, Esteban-Betegón F, Cascales C, Zaldo C, Jezowski A, Stachowiak P. Crystal growth and physical characterization of monoclinic $\text{Li}_3\text{Lu}_3\text{Ba}_2(\text{MoO}_4)_8$. A spectrally broadened disordered crystal for ultrafast mode-locked lasers. Cryst Growth Des. 2012;12(8):3878–3887. doi:10.1021/cg300105g
- Verma A, Sharma SK. Downshifting and up-conversion luminescent properties of triple molybdate NaCa -

- La(MoO₄)₃:Tb³⁺/Yb³⁺ phosphor for solar cell application. AIP Conf Proc. 2019;2115(1):030562. doi:[10.1063/1.5113401](https://doi.org/10.1063/1.5113401)
13. Savina AA, Solodovnikov SF, Belov DA, Basovich OM, Solodovnikova ZA, Pokholok KV, Stefanovich SYu, Lazoryak BI, Khaikina EG. Synthesis, crystal structure and properties of alluaudite-like triple molybdate Na₂₅Cs₈Fe₅(MoO₄)₂₄. J Solid State Chem. 2014;220:217–220. doi:[10.1002/chin.201446018](https://doi.org/10.1002/chin.201446018)
 14. Savina AA, Solodovnikov SF, Belov DA, Solodovnikova ZA, Stefanovich SYu, Lazoryak BI, Khaikina EG. New alluaudite-related triple molybdates Na₂₅Cs₈R₅(MoO₄)₂₄ (R = Sc, In): synthesis, crystal structures and properties. New J Chem. 2017;41:5450–5457. doi:[10.1039/C7NJ00202E](https://doi.org/10.1039/C7NJ00202E)
 15. Yudin VN, Zolotova ES, Solodovnikov SF, Solodovnikova ZA, Korolkov IV, Stefanovich SY, Kuchumov BM. Synthesis, structure, and conductivity of alluaudite-related phases in the Na₂MoO₄–Cs₂MoO₄–CoMoO₄ system. Eur J Inorg Chem. 2019;2:277–286. doi:[10.1002/ejic.201801307](https://doi.org/10.1002/ejic.201801307)
 16. Kozhevnikova NM, Kotova IYu. X-ray study of phases of variable-composition M_{1-x}A_{1-x}R_{1+x}(MoO₄)₃, 0 ≤ x ≤ 0.3–0.5 (M = Na, K; A = Mg, Mn, Co, Ni; R = Al, In, Cr, Fe, Sc). Zh Neorg Khim. 2000;45:102–103.
 17. Kotova IY, Belov DA, Stefanovich SY. Ag_{1-x}Mg_{1-x}R_{1+x}(MoO₄)₃ Ag⁺-conducting nasicon-like phases, where R = Al or Sc and 0 ≤ x ≤ 0.5. Russ J Inorg Chem. 2011;56:1189–1193. doi:[10.1134/S00036023611080122](https://doi.org/10.1134/S00036023611080122)
 18. Grossman VG, Bazarova JG, Molochev MS, Bazarov BG. New triple molybdate K₅ScHf(MoO₄)₆: synthesis, properties, structure and phase equilibria in the M₂MoO₄–Sc₂(MoO₄)₃–Hf(MoO₄)₂ (M = Li, K) systems. J Solid State Chem. 2020;283:121143. doi:[10.1016/j.jssc.2019.121143](https://doi.org/10.1016/j.jssc.2019.121143)
 19. Spiridonova TS, Solodovnikov SF, Savina AA, Kadyrova YuM, Solodovnikova ZA, Yudin VN, Stefanovich SYu, Khaikina EG. New triple molybdate Rb₂AgIn(MoO₄)₃: synthesis, framework crystal structure and ion transport behavior. Acta Crystallogr C. 2018;74(12):1603–1609. doi:[10.1107/S2053229618014717](https://doi.org/10.1107/S2053229618014717)
 20. Spiridonova TS, Solodovnikov SF, Savina AA, Kadyrova YuM, Solodovnikova ZA, Yudin VN, Stefanovich SYu, Kotova IYu, Khaikina EG, Komarov VYu. Rb_{9-x}Ag_{3+x}Sc₂(WO₄)₉: a new glaserite-related structure type, rubidium disorder, ionic conductivity. Acta Crystallogr. B. 2020; 76:28–37. doi:[10.1107/S2052520619015270](https://doi.org/10.1107/S2052520619015270)
 21. Spiridonova TS, Solodovnikov SF, Molochev MS, Solodovnikova ZA, Savina AA, Kadyrova YuM, Sukhikh AS, Kovtunets EV, Khaikina EG. Synthesis, crystal structures, and properties of new acentric glaserite-related compounds Rb₇Ag_{5-3x}Sc_{2+3x}(XO₄)₉ (X = Mo, W). J Solid State Chem. 2022;305:122638. doi:[10.1016/j.jssc.2021.122638](https://doi.org/10.1016/j.jssc.2021.122638)
 22. Basovich OM, Uskova AA, Solodovnikov SF, Solodovnikova ZA, Khaikina EG. Phase formation in the systems Na₂MoO₄–Cs₂MoO₄–Ln₂(MoO₄)₃ and the crystal structure of the new ternary molybdate Cs₇Na₅Yb₂(MoO₄)₉. Vestn Buryats Gos Univ Khim Fiz. 2011;3:24–29. Russian.
 23. ICDD PDF-2 Database, Cards № 01-074-2369, 00-012-0773, 00-024-0958, 01-073-2342, 01-072-2078, 01-089-4691
 24. Smith GS, Snyder RL. F_N: A criterion for rating powder diffraction patterns and evaluating the reliability of powder-pattern indexing. J Appl Crystallogr. 1979;12:60–65.
 25. Rietveld HM. A profile refinement method for nuclear and magnetic structures. J Appl Crystallogr. 1969;2:65–71. doi:[10.1107/S0021889869006558](https://doi.org/10.1107/S0021889869006558)
 26. Bruker AXS TOPAS V4: General profile and structure analysis software for powder diffraction data. User's Manual. Bruker AXS, Karlsruhe, Germany. 2008.
 27. Järvinen M. Application of symmetrized harmonics expansion to correction of the preferred orientation effect. J Appl Crystallogr. 1993;26(4):525–531. doi:[10.1107/S0021889893001219](https://doi.org/10.1107/S0021889893001219)
 28. WebCSD. Available from:<https://www.ccdc.cam.ac.uk/structures/>
 29. Okada K, Otsuka J. Structures of potassium sodium sulphate and tripotassium sodium disulphate, Acta Crystallogr. 1980;36:919–921. doi:[10.1107/S0567740880004852](https://doi.org/10.1107/S0567740880004852)